Natively Folded HypF-N and Its Early Amyloid Aggregates Interact with Phospholipid Monolayers and Destabilize Supported Phospholipid Bilayers

Claudio Canale,* Silvia Torrassa,* Pasquale Rispoli,* Annalisa Relini,* Ranieri Rolandi,* Monica Bucciantini,†‡ Massimo Stefani,†‡ and Alessandra Gliozzi*

*Department of Physics, University of Genoa, Genoa, Italy; and †Department of Biochemical Sciences, and ‡Research Centre on the Molecular Basis of Neurodegeneration, University of Florence, Florence, Italy

ABSTRACT Recent data depict membranes as the main sites where proteins/peptides are recruited and concentrated, misfold, and nucleate amyloids; at the same time, membranes are considered key triggers of amyloid toxicity. The N-terminal domain of the prokaryotic hydrogenase maturation factor HypF (HypF-N) in 30% trifluoroethanol undergoes a complex path of fibrillation starting with initial 2–3-nm oligomers and culminating with the appearance of mature fibrils. Oligomers are highly cytotoxic and permeabilize lipid membranes, both biological and synthetic. In this article, we report an in-depth study aimed at providing information on the surface activity of HypF-N and its interaction with synthetic membranes of different lipid composition, either in the native conformation or as amyloid oligomers or fibrils. Like other amyloidogenic peptides, the natively folded HypF-N forms stable films at the air/water interface and inserts into synthetic phospholipid bilayers with efficiencies depending on the type of phospholipid. In addition, HypF-N prefibrillar aggregates interact with, insert into, and disassemble supported phospholipid bilayers similarly to other amyloidogenic peptides. These results support the idea that, at least in most cases, early amyloid aggregates of different peptides and proteins produce similar effects on the integrity of membrane assembly and hence on cell viability.

INTRODUCTION

Amyloid aggregates are oligomers or polymeric fibrillar assemblies formed by a number of structurally different peptides and proteins either in vitro or in vivo. The intracellular or extracellular deposition of these assemblies represents the main hallmark of amyloid diseases (1). Currently, amyloid aggregates, particularly in their prefibrillar oligomeric organization, are considered the main culprit of cell impairment and death resulting in tissue damage and eventually in the appearance of the clinical symptoms of the different amyloidoses (2).

Since 1998, it has increasingly been recognized that the ability to generate amyloid assemblies is a generic property of polypeptide chains (reviewed in Dobson (2)); general consensus has also been reached on the idea that amyloid cytotoxicity, at least in most cases, involves precursors of mature fibrils and is a generic property of these assemblies not associated with specific amino acid sequences (2,3). These remarkable results have considerably increased the number of peptides and proteins one can study as models to investigate the general basic features underlying protein aggregation and aggregate toxicity. They have also led to reconsideration of the importance of the structural adaptations of natural polypeptide chains that evolved to avoid the appearance of aggregation-prone sequences (4,5). The cellular tools, including molecular chaperones and the ubiquitin proteasome pathway of protein degradation, have also been considered for their ability to enable cells to cope with the appearance of misfolded proteins or their early aggregates (6).

Much remains to be understood about the biochemical and molecular features underlying protein aggregation and aggregate cytotoxicity; however, increasing consensus has been gained on the key role performed in most cases by biological surfaces, particularly cell membranes, both as triggers of protein/peptide aggregation and as primary targets of prefibrillar amyloid aggregates. Indeed, surfaces, either synthetic (mica, SDS micelles, lipid vesicles) (7–9) or biological (cell membranes, RNA, glycosaminoglycans, collagen) (10–14), are increasingly considered key sites where proteins and peptides can be recruited, increasing their local concentration, undergoing misfolding, or, when unfolded, organizing into beta structures, with subsequent oligomerization and amyloid nucleation (15). According to the amyloid channel hypothesis, first proposed in 1993 (16), amyloid aggregate toxicity arises from the nonspecific permeabilization of the cell membrane after interaction with the aggregates, with disruption of the ion balance across the membrane and cell impairment leading to cell death. Presently, the channel hypothesis is supported by a large number of reports depicting cell membranes, particularly the plasma membrane, as the primary site of the interaction of cell components with intracellular or extracellular aggregates.

Protein/peptide interaction with membranes or other surfaces can result in structural changes favoring misfolding of the polypeptide chain and aggregate nucleation (17–19).

Submitted May 23, 2006, and accepted for publication August 22, 2006.

Address reprint requests to Prof. Alessandra Gliozzi, Dept. of Physics, University of Genoa, Via Dodecaneso 33, I-16146 Genoa, Italy. Tel.: 39-010-3536221; Fax: 39-010-314218; E-mail: gliozzi@fisica.unige.it; or Prof. Massimo Stefani, Dept. of Biochemical Sciences, University of Florence, V. le Morgagni 50, 502134 Florence, Italy. Tel.: 39-055-4598307; Fax: 39-055-4598905; E-mail: stefani@scibio.unifi.it.

0006-3495/06/12/4575/14 $2.00

doi: 10.1529/biophysj.106.089482

Membrane-induced protein unfolding and the interaction with membranes of misfolded or unfolded polypeptides or their early aggregates may depend on several factors. The presence of strong local electrostatic fields on the membranes can weaken polar interactions populating protein folds where nonnative interactions are favored. In addition, misfolded proteins, unfolded peptides, or their early aggregates are destabilized by exposure to the aqueous phase of hydrophobic patches or backbone hydrogen bonds and can gain stability partitioning into the nonpolar membrane environment (20). On the other hand, the ability of proteins/peptides or their early aggregates to interact with membranes depends on chemical and physicochemical features of the membrane itself, including curvature, fluidity or rigidity, and lipid composition (21–23). In this respect, lipid components may play a major role. For example, it is increasingly reported that anionic lipids can favor membrane-induced protein misfolding and subsequent aggregate nucleation as well as prefibrillar aggregate interaction with the membrane (24–26). The cholesterol content of the membrane has also been reported to affect the way peptides or proteins (27) or their early aggregates (22,28) interact with the membrane, as well as their ability to cross the membrane and to penetrate inside cells (29,30). Taken together, these data justify efforts to describe in detail the molecular and physicochemical features underlying the interaction of proteins, peptides, and their early aggregates with lipid membranes, both synthetic and biological.

The N-terminal domain of the bacterial hydrogenase maturation factor HypF (HypF-N) was previously characterized both structurally and with regard to its folding and unfolding behavior (31). It belongs to the acylphosphatase family, though it is devoid of acylphosphatase activity; in fact, it is an α/β protein with a central twisted five-stranded β-sheet faced by two antiparallel α-helices, with strands arranged in the same 4-1-3-2-5 topology as that of any other acylphosphatase (32). The similarity to the members of the acylphosphatase family is confirmed by the presence in the sequence of the two conserved residues that are involved in catalysis in all active acylphosphatases, namely Arg-23 and Asn-41, and by ~34% amino acid identity with respect to the eukaryotic acylphosphatases, with a higher occurrence of hydrophobic residues and a lower isoelectric point.

In this study, we investigated the surface properties and lipid-peptide interactions of the natively folded monomeric HypF-N and its early aggregates. HypF-N early aggregates were previously shown to interact with, and to permeabilize, cell membranes and to impair cell viability, like many peptides and proteins associated with amyloid diseases (3,29,33). The data reported in this study show that HypF-N forms stable films at the air/water interface, similarly to Aβ peptides (34,35), and is able to insert into synthetic phospholipid bilayers. HypF-N prefibrillar aggregates are also able to destabilize supported phospholipid bilayers as human amylin (36).

EXPERIMENTAL PROCEDURES

Materials

Bovine brain phosphatidylserine (PS), egg-yolk phosphatidylcholine (PC), trifluoroethanol (TFE), dithiothreitol, and ammonium acetate were obtained from Sigma Aldrich (St. Louis, MO). Water was purified by using a Milli-Q system (Millipore, Bedford, MA) yielding a water resistivity value higher than 18 MΩ·cm. The recombinant N-terminal domain of the bacterial hydrogenase maturation factor HyPF was purified from an *Escherichia coli* expression system, as reported previously (37). Aggregation of HypF-N was achieved by incubating the protein at room temperature at a concentration of 0.3 mg/ml in 30% (v/v) TFE, 1.0 mM dithiothreitol, and 20 mM ammonium acetate, pH 5.5. Rabbit anti-HypF-N polyclonal antibodies were provided by Primm S.r.l. (Milan, Italy); Alexa-488-conjugated anti-rabbit IgG secondary antibodies colloidal gold complexes (colloidal gold size, 10 nm) were purchased from Molecular Probes (Eugene, OR).

Measurements at the air/water interface

HypF-N partitioning at the air/water interface was studied by monitoring the surface pressure of a water solution after protein injection. The measurements were made using three 100-ml home-built teflon Langmuir troughs with three different surface areas: 48.6 cm^2, 81.6 cm^2, and 115.6 cm^2. The protein was injected into the water subphase and the surface pressure was measured at different times using a NIMA ST9000 pressure sensor (Nima Technology, Warwick, UK), while allowing the system to reach equilibrium. Surface pressure-area isotherms were measured in an R&K trough (Potsdam, Germany) at a barrier compression speed of 4.5 cm^2/min. Typically, 60 μl of a 0.3-mg/ml HypF-N solution were injected into a water subphase 25 ml in volume; the isotherm was measured after protein partitioning at the air/water interface. Measurements in the presence of lipid monolayers were performed by forming a lipid monolayer on the subphase surface already containing the protein at the desired concentration. Monolayers were formed by spreading an aliquot of lipid solution (typically 10 μl of a 0.5-mg/ml solution) using a Hamilton microsyringe. Surface pressure-area isotherms were measured as described above.

Atomic force microscopy

Atomic force microscopy (AFM) measurements were performed with a Nanoscope IIIa Dimension 3000 scanning probe microscope (Digital Instruments, Santa Barbara, CA) equipped with a G scanning head (maximum scan size, 100 $\times$ 100 μm). Images were acquired in tapping mode in fluid using 200-μm gold-coated silicon nitride V-shaped cantilevers (Veeco Instruments, Santa Barbara, CA) with nominal spring constant of 0.06 N/m equipped with either a standard or an oxide-sharpened tip. The drive frequency was between 4.5 and 6.0 kHz, the drive amplitude betweeen 18 and 20 V, and the scan rate between 0.5 and 1.0 Hz. Images were collected with 512 data points per line. Since the object size in the image plane can be broadened by tip-size effects, the apparent size deduced visually from the image can be overestimated; only the *Z* scale, reported in the figure legends as *z* range and encoded in the image colors, should be considered to assess the real object size.

Measurements of the bilayer step height were obtained from the height in cross section of the AFM images. The data reported (see histograms in Figs. 7 and 8) represent relative heights (the height of a step measured with respect to the adjacent one) and were obtained from at least five images corresponding to different regions of two different samples. For each histogram, the corresponding set of images had scan areas ranging from 1.5 to 5 μm.

Preparation of supported lipid bilayers

Unilamellar vesicles were prepared using bovine brain PS or egg-yolk PC (Sigma-Aldrich, Darmstadt, Germany). The lipid was hydrated at a

concentration of 1.0 mg/ml in 20 mM acetate buffer, pH 7.4, with the aid of an ultrasonic bath (ACAD, Genoa, Italy) for 10 min. Then the sample was sonicated with a tip sonicator (Ultrasonics Ltd., Northants, UK) for ~15 min. To prevent overheating, every 2.0 min, sonication was stopped for 1.0 min. To remove large lipid aggregates and titanium impurities released by the tip, the suspension was centrifuged for 10 min at 11,500 × *g* in a Sorvall RC-SB Superspeed Centrifuge (Du Pont Instruments, Newton, CT). Supported lipid bilayers were prepared via vesicle fusion on freshly cleaved mica substrates. The liposome solution was incubated on the mica surface at room temperature for 1.0 h, then the sample was rinsed and the bilayers were imaged in aqueous solution.

To test the HypF-N-lipid membrane interaction, aliquots of the protein sample (typically 60 μl adjusted to pH 7.4) were withdrawn at different aggregation times and deposited on supported lipid bilayers obtained as described above. To eliminate TFE, which could give rise to artifacts, before deposition on the supported lipid bilayer the volume of protein samples was reduced to 70% of its initial value by evaporation under a stream of nitrogen and then restored to 100% by adding buffer without TFE. Mass spectrometry measurements showed that after this treatment, the amount of TFE still present in the protein solution was ~1%. The final protein concentration on the supported lipid bilayer was 7.6 μM, as a result of a further 3:1 dilution with buffer; this corresponds to a final TFE concentration of <0.3%. After 20 min of incubation with the protein, the supported lipid bilayers were rinsed and imaged in water solution. HypF-N incorporation into the lipid phase was checked by incubating the samples at room temperature for 20 min with 50 μl of rabbit anti-HypF-N polyclonal antibodies diluted 1:100. After rinsing with water, the sample was incubated at room temperature for 20 min with 50 μl of colloidal gold complexed with anti-rabbit IgG antibodies (1:200 dilution), rinsed with water and imaged under liquid. Each step of this procedure was carried out taking care to avoid sample dehydration.

RESULTS

Pure HypF-N monolayers

It has previously been shown that HypF-N unfolded in 30% TFE undergoes fibrillation, producing oligomers that are able to interact and permeabilize synthetic lipid vesicles and cell membranes (29,38). This led us to investigate the features of the interaction of HypF-N with different surfaces to provide information on the possible effect of surfaces in favoring domain misfolding and aggregation. We initially investigated the surface activity of natively folded HypF-N by testing its ability to partition at the air/water interface. To this purpose, we used three home-built teflon Langmuir troughs with different surface areas and the same subphase volume, as detailed in Experimental Procedures. Surface pressure increased with time after injection of native monomeric HypF-N into ultra pure water at a nominal bulk concentration in the 70- to 100-nM range, approaching a limiting value (Fig. 1 *a*). This finding indicates that HypF-N molecules assemble into a monolayer at the air/water interface. Interestingly, at a fixed protein concentration (70 nM), the limiting pressure values were slightly but significantly increased (14, 16, and 18 mN/m, respectively) with the trough area (data not shown). Fig. 1 *b* shows a typical pressure-area isotherm obtained 1.0 h after injecting natively folded

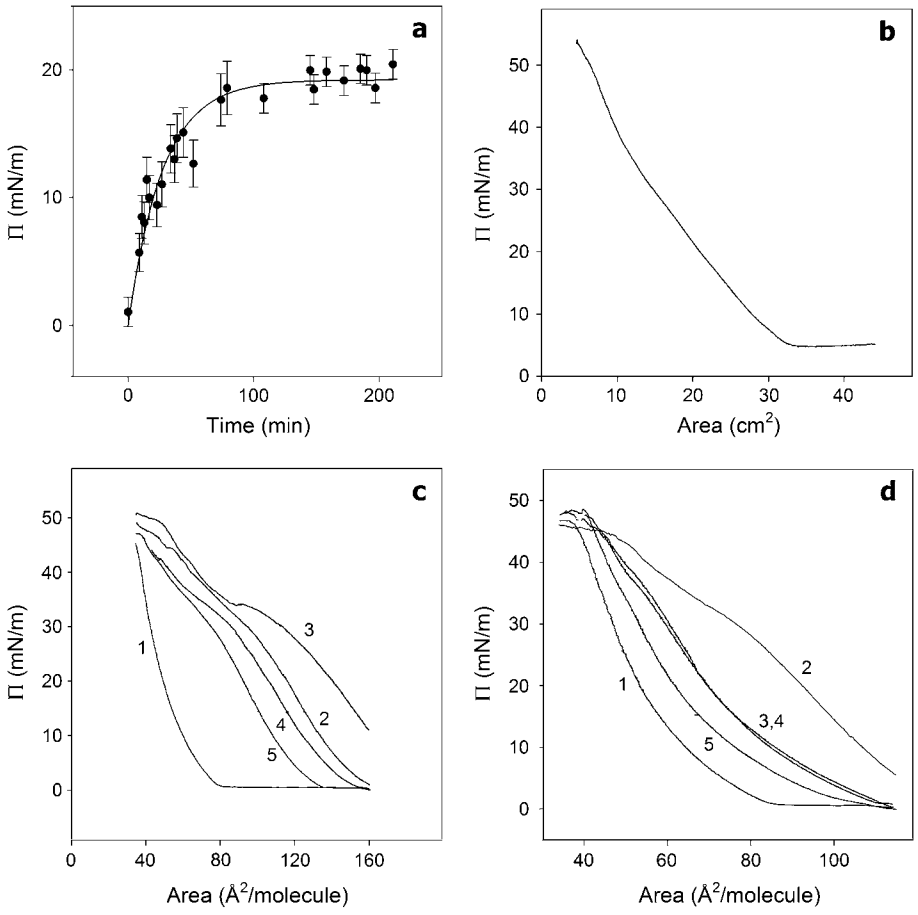

FIGURE 1 (*a*) Adsorption isotherm of HypF obtained at a protein concentration of 100 nM at a surface area of 48.6 cm^2. (*b*) Pressure-area isotherm of HypF-N. (*c* and *d*) Pressure-area isotherms of PS (*c*) and PC (*d*) monolayers without HypF-N (*1*); in the presence of native HypF-N (*2*); and in the presence of HypF-N at aggregation times of 2 h (*3*), 24 h (*4*), and 48 h (*5*).

monomeric HypF-N into the water subphase. The isotherm displays a wide region of linear behavior and a nonzero surface pressure (around 5.0 mN/m) at the maximum area available, due to protein adsorption at the air/water interface. The protein film could be compressed to a surface pressure >50 mN/m before collapsing.

Insertion of HypF-N into lipid monolayers

We also investigated the surface pressure of lipid monolayers after the insertion of HypF-N either in the monomeric state or in different prefibrillar aggregated states obtained by incubating the protein in the presence of 30% TFE for different aggregation times. In a previous report we showed that HypF-N incubated in the presence of 30% TFE undergoes a complex path of aggregation starting with globules 2–5 nm in diameter. After three days of aggregation the globular material appears to be assembled into thin crescents, which then develop into closed rings with a diameter of ~1 μm and subsequently organize into ribbonlike fibrils. The first twisted fibrils (mean fibril size, 8.5 nm; axial repeat period, ~70 nm) appear after five days of incubation. The fibril size displays a broad distribution, probably reflecting different numbers of constituent protofilaments and further association of fibrils to form larger supercoiled structures (38).

In this study, to rule out artifacts arising from the presence of TFE, we performed control experiments on water subphases containing the same amount of TFE present in the protein aggregates. No increase in surface pressure was detected as a function of time at a fixed surface area. Upon compression, the pressure-area isotherm of pure phospholipid monolayers was slightly shifted toward larger areas. Therefore, the isotherms obtained in the presence of the protein were always compared with the corresponding pure lipid isotherm recorded in the presence of TFE.

A surface pressure increase from 0 to 10 mN/m was measured in PS monolayers formed on a subphase containing HypF-N aged 2.0 h in TFE (where only 2- to 5-nm globules are present), with the trough barriers completely open (Fig. 1 *c*, *curve 3*). Instead, the initial increase of surface pressure was almost negligible (~1.0 mN/m) in the presence of natively folded monomeric HypF-N (Fig. 1 *c*, *curve 2*). Such a difference in surface pressure in the presence of the same amount of HypF-N indicates that more HypF-N molecules were incorporated in the monolayer when added as initial aggregates than as natively folded monomers. Alternatively, it could be proposed that the initial aggregates correspond to partially unfolded and less densely packed molecules; these would occupy a larger surface area than the natively folded counterparts as a result of either their increased molecular volume or, possibly, further unfolding at the PS/water interface. No increase of surface pressure at trough barriers completely open was found using subphases containing HypF-N incubated in TFE for longer time periods (24 h and 48 h), where higher-order oligomers and polymers are present (Fig. 1 *c*, *curves 4* and *5*). This finding can be explained by considering that these higher-order oligomers could occupy slightly less surface area in the PS monolayer than that occupied by the same amount of natively folded molecules; they could also resist further unfolding of the constituting monomers at the PS/water interface, thus occupying a considerably reduced surface area with respect to that covered by the same amount of misfolded protein. Similar considerations could explain the shift of the area/molecule corresponding to the onset of a surface pressure from 80 Å^2/molecule in the absence of the protein (Fig. 1 *c*, *curve 1*) to 155 or 135 Å^2/molecule in the presence of protein aggregates aged for 24 h (*curve 4*) or 48 h (*curve 5*), respectively.

The change in surface area upon monolayer compression was larger in the presence of HypF-N in the natively folded, monomeric state (Fig. 1 *c*, *curve 2*) or incubated in TFE for short times (Fig. 1 *c*, *curve 3*). Instead, the mature fibrils, considered the stable end-product of the aggregation process, were substantially unable to insert into the lipid monolayer and their presence did not modify the curve registered in the absence of HypF-N (not shown). In addition, the shape of the isotherms appears completely different in the presence or in the absence (Fig. 1 *c*, *curve 1*) of monomeric or aggregated HypF-N, respectively, as indicated by the marked inflection at ~30 mN/m in the curves measured in the presence of the protein; the latter finding can be interpreted as a consequence of the expulsion of the protein, or its early aggregates, from the compressed lipid film.

A marked expansion of the isotherm with nonzero surface pressure at maximum trough surface area was found after insertion of monomeric HypF-N into pure PC monolayers (Fig. 1 *d*, *curve 2*); the insertion of HypF-N prefibrillar aggregates caused an expansion of the isotherm, although to a lesser extent than with PS monolayers, indicating that the latter can host a larger amount of protein or, alternatively, that the hosted protein molecules are less compact and occupy a larger surface area. With PC monolayers, the area per molecule corresponding to the onset of a nonzero surface pressure was shifted from 85 Å^2/molecule in the absence of HypF-N (*curve 1*), to ~110 Å^2/molecule in the presence of HypF-N aggregates (Fig. 1 *d*, *curves 3–5*). These values are significantly lower than those determined under the same conditions with PS monolayers (Fig. 1 *c*, *curves 2*, *4*, and *5*), indicating a reduced ability of HypF-N and its early aggregates to insert into the PC monolayer as compared with the PS one.

The reduced effect on the lipid monolayers produced by the presence of protein aggregates was confirmed by the shape of the isotherms. Indeed, PS monolayers were more heavily modified than PC monolayers. In particular, PC monolayers formed on a subphase with HypF-N incubated with 30% TFE for 2.0 h or 24 h (Fig. 1 *d*, *curves 3* and *4*) still showed the inflection at 30 mN/m, although the latter appeared less marked than that found with PS monolayers; instead, in the

presence of HypF-N aged for 48 h, the shape of the isotherm became closely similar to that of the pure lipid, though shifted to larger molecular areas (Fig. 1 *d*, *curve 5*).

The results of the experiments carried out on phospholipid monolayers indicate that HypF-N prefibrillar aggregates display the tendency to partition in the lipid moiety with different efficiency and, possibly, different conformational features depending on the type of lipid and the state of aggregation of the protein. Overall, these data suggest that natively folded HypF-N and its prefibrillar aggregates interact with, and insert into, PC and PS monolayers. Our data also indicate that monomeric HypF-N and its early prefibrillar aggregates, consisting of small (~2–5 nm in height) globular entities, interact more efficiently with monolayers than do more aged aggregates, where higher-order oligomeric and polymeric forms are present.

AFM imaging of supported lipid bilayers interacting with HypF-N aggregates

We subsequently investigated the possible structural changes occurring in lipid bilayers upon protein insertion. To this purpose, the interaction of supported lipid bilayers with HypF-N incubated in 30% TFE for different time periods was studied by AFM. A supported lipid bilayer can be produced by depositing a drop of liposome suspension on freshly cleaved mica; as a consequence, liposomes may adsorb onto the substrate and spontaneously coalesce, forming a bilayer (39). Fig. 2 shows the typical morphology of a supported lipid bilayer obtained upon deposition onto mica of PC (Fig. 2 *a*) or PS (Fig. 2 *b*) liposomes. PC liposomes generate a rather uniform bilayer membrane displaying relatively moderate defects (the darker areas in Fig. 2 *a*) with maximum depth of ~4.5 nm (the typical thickness of a bilayer). In the case of PS bilayers, membrane defects were usually much wider (Fig. 2 *b*), with depths corresponding to the thickness of a bilayer (see Fig. 9 *a*); in some cases, the membrane appeared fragmented into islands with the typical thickness of a bilayer. Similar morphologies were previously reported for mica-supported phospholipid bilayers (40). The differences in bilayer morphology are likely to be due to electrostatic effects determined by the ionic strength and pH required in these experiments. We observed that at higher ionic strength, the coverage of mica by lipid bilayers turns out to be almost complete (data not shown). Despite the observed variability of the morphology of pure PS bilayers, the changes induced as a consequence of membrane-protein interaction are always clearly detectable and unambiguous.

As already observed for lipid monolayers, even in the case of supported lipid bilayers the structure of the membrane was strongly affected by exposure to native monomeric HypF-N. Fig. 3 shows typical images obtained after incubation of PC or PS bilayers with 7.0 μM natively folded, monomeric HypF-N for 20 min. Small, fragmented domains were seen in PC bilayers, with the background displaying a widespread

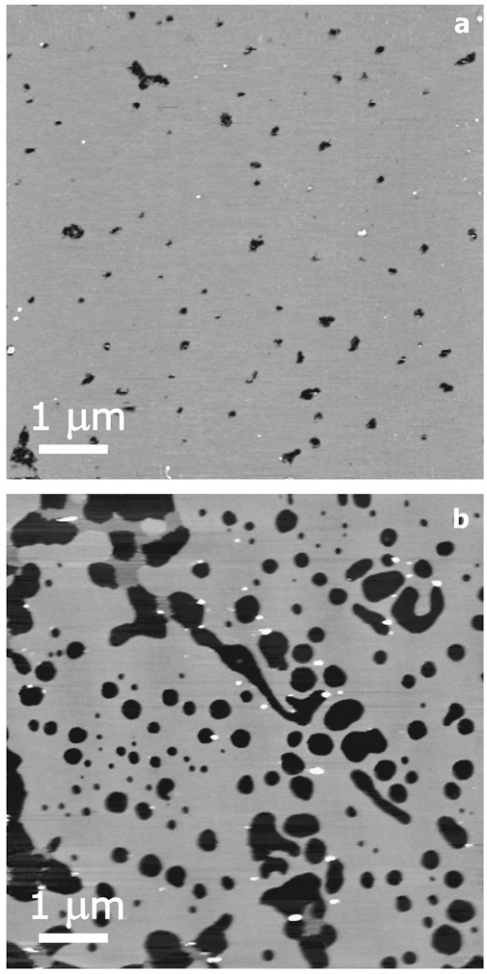

FIGURE 2 Tapping-mode atomic force microscopy images (height data) of supported membranes made of (*a*) PC and (*b*) PS. Scan size, 7.5 μm; *z* range, 20 nm.

granular appearance (Fig. 3 *a*) similar to that obtained previously using amylin (36). The domains often appear located on previous membrane defects, indicating that the latter are preferential sites for membrane rearrangement. Fragmentation occurred also in PS membranes; in this case the background was flat, since it corresponded to bare mica, as shown by the scratch made with the AFM tip in the middle of the image (Fig. 3 *b*).

To test whether the dramatic change in bilayer morphology in the presence of native HypF-N resulted from direct insertion of the protein into the lipid layer, after treatment with HypF-N we incubated PC and PS supported bilayers with rabbit anti-HypF-N antibodies and then with anti-rabbit Ig antibodies conjugated to 10 nm colloidal gold beads. A rather uniform nanoparticle distribution on the sample surface (corresponding to a measured surface density of 44 μm^{-2} and 18 μm^{-2} for PC or PS membranes, respectively), with nearly absent particle clusters, was observed by AFM (Fig. 4 *a*). Such a measurement of nanoparticle surface

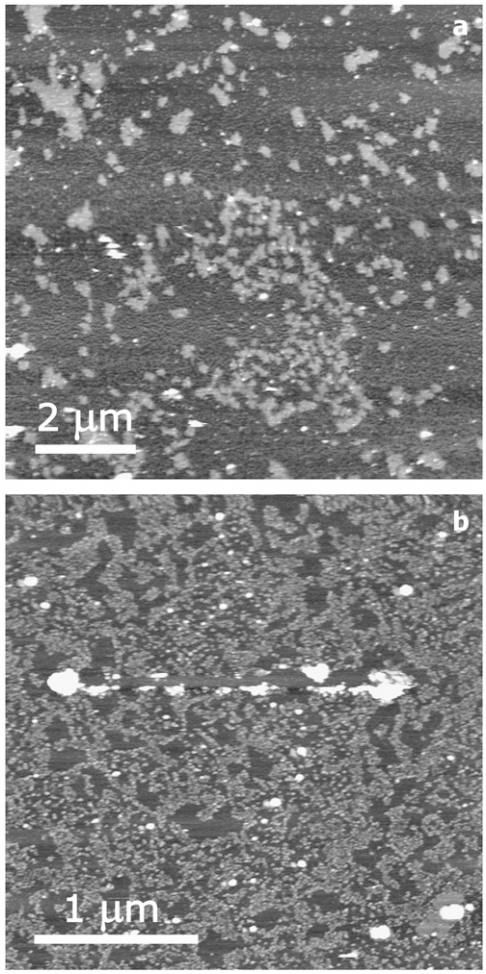

FIGURE 3 Tapping-mode atomic force microscopy images (height data) of supported membranes made of (*a*) PC and (*b*) PS after incubation with native HypF-N. Scan sizes: (*a*) 10 μm; (*b*) 3 μm; *z* range, 20 nm.

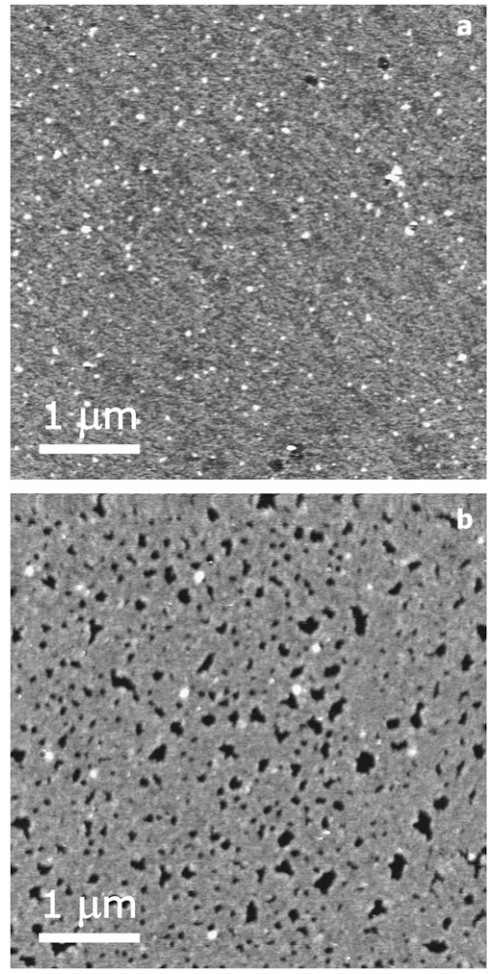

FIGURE 4 Detection of membrane-incorporated HypF-N by colloidal gold -antibody binding (details in the text): tapping-mode atomic force microscopy images (height data) of PC-supported membranes: (*a*) treated with native HypF-N; (*b*) control, in the absence of HypF-N. Scan size, 5.0 μm; *z* range, 20 nm.

density could underestimate the actual amount of protein inserted in the PC bilayer; in fact, the efficiency of antibody binding to HypF-N could be much less than 100% due to both reduced epitope accessibility and conformational changes in the protein partitioned into the lipid moiety. On the other hand, the amount of lipid-associated protein could also have been overestimated due to nonspecific Ig adsorption to the lipid bilayer. To rule out such a possibility, the same measurements were made incubating the bilayers with Ig in the absence of HypF-N (Fig. 4 *b*). Under these conditions, nanoparticle surface densities of only 3.4 and 1.6 μm^{-2} were found for PC and PS bilayers, respectively, and the bilayers remained substantially intact. We also used phase imaging (41–43) to check whether protein adsorption/insertion into the bilayer could give rise to local changes of viscoelastic properties. However, in our experimental conditions the analysis of the phase-contrast signal did not reveal either membrane stiffness changes or the presence of the protein in PS and PC lipid bilayers.

AFM images of PC- and PS-supported bilayers exposed for 20 min to HypF-N previously incubated for 24 h in 30% TFE, are reported in Fig. 5, *a* and *c*, respectively. The morphology of PC membranes did not change substantially in the presence of the aggregates with respect to that imaged in their absence (Fig. 2 *a*); however, the depth of the defects decreased, and small domains appeared on the surface of the membranes exposed to the aggregates. The morphological features of similarly treated PS membranes (Fig. 5 *c*) also resembled those imaged in the absence of the protein (Fig. 2 *b*); however, in this case a coexistence of areas still homogeneous with areas clearly displaying membrane disruption was apparent. The inset in Fig. 5 *c* shows details of the disrupted regions. Membrane disruption increased after exposure of the supported bilayers for 20 min to HypF-N preaggregated for 48 h in TFE (Fig. 5, *b* and *d*). In both cases, membranes were fragmented into domains with

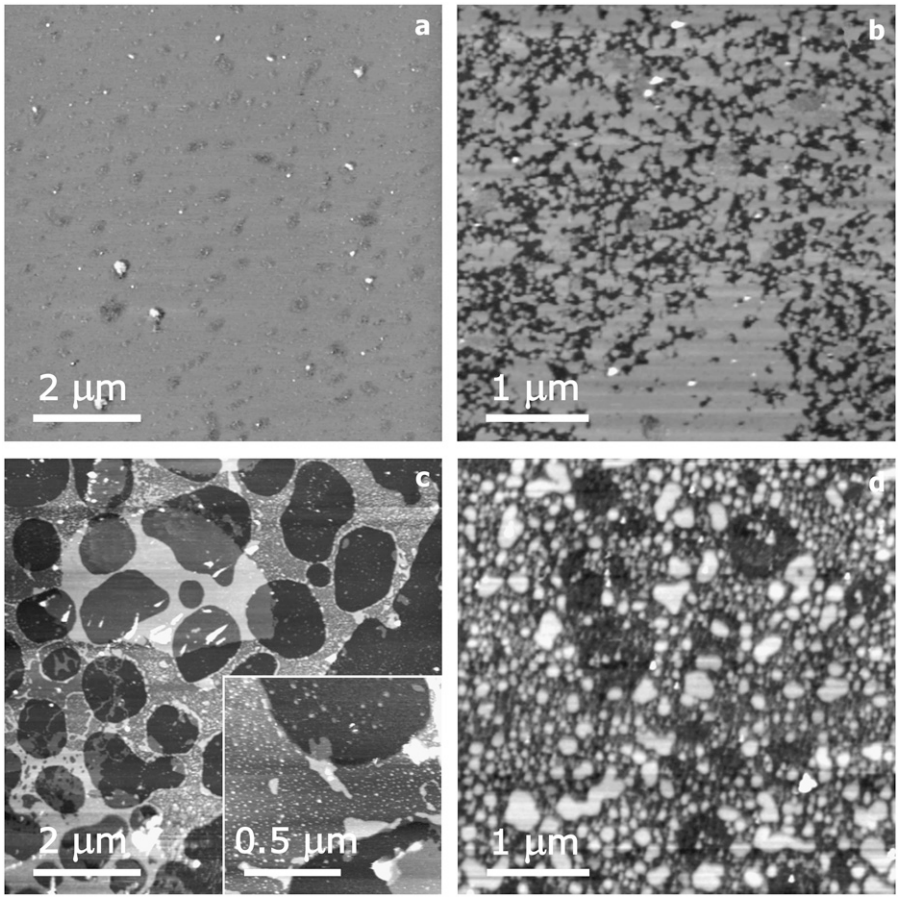

FIGURE 5 Tapping-mode atomic force microscopy images (height data) of supported membranes made of (*a* and *b*), PC and (*c* and *d*) PS after incubation with HypF-N preaggregated for 24 h(*a* and *c*) and 48 h (*b* and *d*). Scan sizes: (*a*) 8.2 μm, (*b*) 4.3 μm, and (*c*) 8.2 μm, inset 1.2 μm; (*d*) 4.3 μm; *z* range, 20 nm.

typical sizes of a few hundreds of nanometers, whereas intact bilayer regions were not observed anymore.

The AFM images in Fig. 6 show the morphologies of supported PC membranes not exposed to the protein (Fig. 6 *a*) or exposed for 20 min to HypF-N aggregates obtained by 72 h incubation in 30% TFE after washing out the remaining soluble monomeric protein. These aggregates were previously shown to consist mainly of large rings made of globular particles (38). Under these conditions, 0.7- to 1.0-nm steps were formed in the supported bilayers while the hole depth decreased from that corresponding to the thickness of a bilayer to ~2–3 nm. In addition, regions displaying membrane disruption and granular appearance were observed (Fig. 6 *b*). Although the step height was constant with time, the size of the low-thickness domains increased, as shown in Fig. 6, *c* and *d*. These results indicate that membrane rearrangements triggered by lipid-protein interactions still take place, even in the absence of a protein reservoir in the aqueous phase. It is likely that bilayer plasticity is greatly increased upon protein insertion; in addition, since domains grow rather uniformly in all directions on the sample surface, the growth process does not seem to be facilitated by sample scanning by the tip.

Figs. 7 and 8 display the quantitative analysis of the changes in membrane surface morphology as determined by AFM imaging. Fig. 7 shows a comparison between the step-height distributions measured for PC membranes in the absence of the protein and after incubation with HypF-N at different aggregation times, respectively. Although in the absence of the protein the distribution peak corresponded to the thickness of a bilayer, incubating the supported membranes in the presence of the protein shifted the distribution to lower values. Such an effect was more evident with protein samples at the very early times of aggregation (Fig. 7 *b*), whereas in the presence of protein left in the aggregation solution for longer times the height distribution became bimodal, with peaks at 4.0 and 2.0 nm (Fig. 7 *c*) or mainly at 2.0 nm (Fig. 7 *d*).

We could not measure the step-height distribution in the presence of natively folded, monomeric HypF-N since at these conditions the PC membranes are almost completely disrupted, resulting in the appearance of granular structures (Fig. 3 *a*). Instead, the height distribution of PS membranes in the presence of monomeric HypF-N (Fig. 8 *b*) was measurable and appeared considerably shifted to values much smaller than those found in the absence of the protein and corresponding to the thickness of a bilayer (Fig. 8 *a*). A similar effect was observed upon exposure of lipid bilayers to HypF-N aggregated for 48 h (Fig. 8 *c*), whereas in the presence of HypF-N aggregated for 72 h a larger spreading

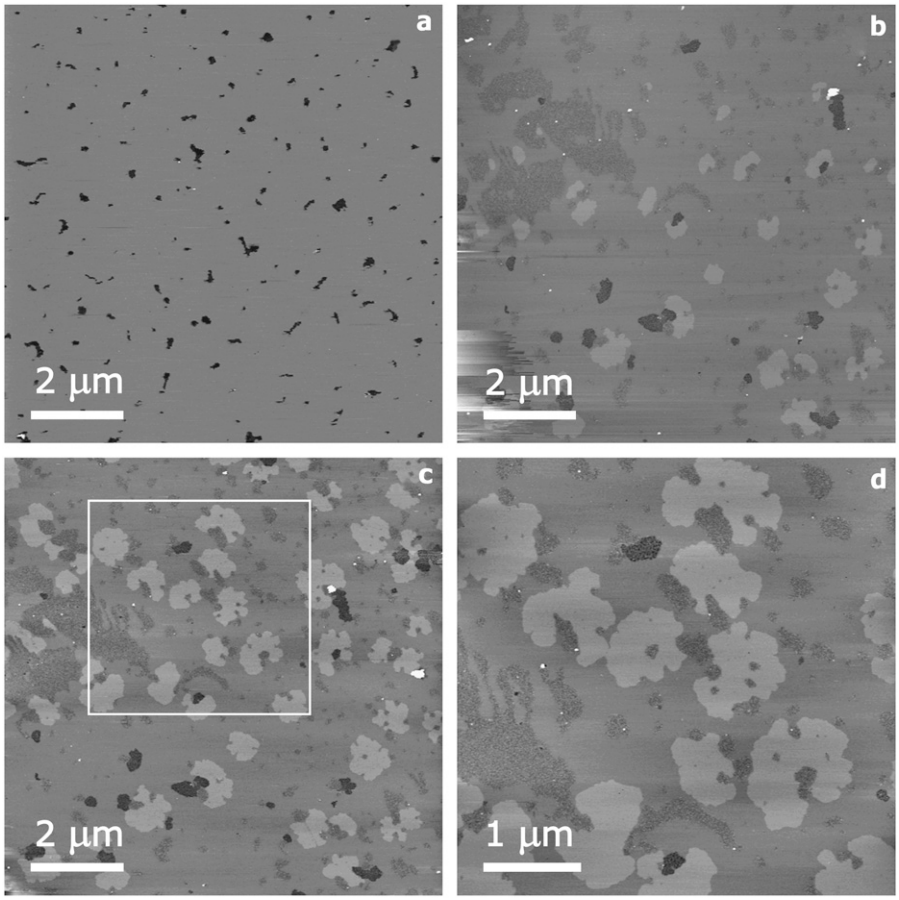

FIGURE 6 Tapping-mode atomic force microscopy images (height data) of supported membranes made of PC. (*a*) PC without HypF-N. (*b–d*) Evolution of surface morphology as a function of time after incubation with HypF-N preaggregated for 72 h. (*b*) $t = 0$. (*c*) $t = 20$ min. (*d*) The area delimited by the square in *c* imaged at $t = 60$ min. Scan sizes: (*a–c*) 10 μm; (*d*) 4.9 μm; *z* range, 20 nm.

of the step values was found (Fig. 8 *d*, *gray*). For PS membranes we also determined the distribution corresponding to an aggregation time of 13 days (Fig. 8 *d*, *cross-hatched bars*), where HypF-N is mostly present as mature amyloid fibrils. Under these conditions the distribution was very similar to that found in the absence of the protein (Fig. 8 *a*), although in the presence of fibrils thin steps are slightly more populated. This suggests that fibrils are not able to disassemble our supported phospholipid bilayers, in agreement with previous data indicating their inability to permeabilize synthetic membranes (38) or to impair cell viability when present in the cell culture medium (3), unless they do not interact with specific membrane proteins, as recently reported for globular and fibrillar mammalian PrP (44). Fig. 9 compares typical surface profiles obtained from image sections taken in the absence (*a*) and in the presence (*b*) of protein aggregates aged 13 days in 30% TFE. These sections clearly show the change from the regular bilayer step pattern observed in the absence of the protein to membrane rearrangement with the formation of thin steps. However, as shown in Fig. 8 *d*, the protein aggregates aged 13 days give rise to a much lower fraction of these steps than the sample incubated for 72 h. This finding suggests a very low membrane destabilization and is in agreement both with the lack of liposome permeabilization by mature HypF-N fibrils, observed previously (38), and with the very small changes recorded in the PS monolayer isotherm in the presence of mature fibrils (data not shown). Sample washing before AFM imaging resulted in the removal of mature fibrils (only a short fibril is visible in the left corner of Fig. 9 *b*), further confirming the weak interaction between fibrils and lipid membranes.

DISCUSSION

Previous reports have shown that in 30% TFE HypF-N undergoes amyloid aggregation (45) through a pathway starting with the appearance of 2.0- to 5.0-nm globular entities and eventually culminating in the appearance of mature amyloid fibrils (38). The prefibrillar assemblies populated in the path of HypF-N fibrillation were also shown to permeabilize phospholipid bilayers enriched in anionic phospholipids (38), to bind to the plasma membrane of cultured cells (30), and to be internalized inside the cytoplasm, resulting in cell impairment and death (29). This behavior is very similar to that reported for prefibrillar aggregates of many other peptides and proteins either associated or not associated with amyloid disease (9,46,47).

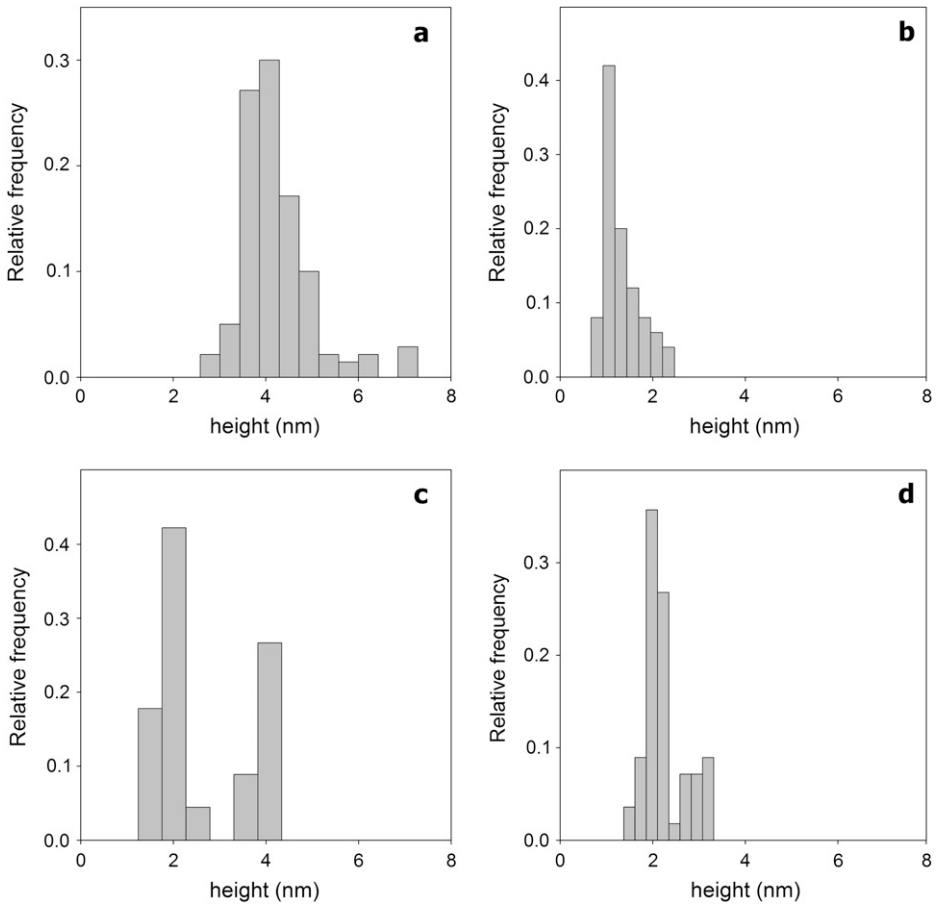

FIGURE 7 Histogram of PC membrane step height measured from surface profiles (*a*) without HypF-N and (*b–d*) after incubation with HypF-N aggregated for 3 h, 48 h, and 72 h, respectively.

The mechanisms underlying the cytotoxic effects of amyloid oligomers can be elucidated by studying the interaction between these oligomers and model membranes such as phospholipid monolayers and supported bilayers. Previous studies have shown that the permeabilization of synthetic membranes by amyloidogenic peptides may be traced back to the generation of defects in the lipid bilayer; these appear to result from membrane disassembly with lateral cohesive force reduction rather than from the presence of well-defined oligomeric channels spanning the membrane (34,36). Therefore, to better assess the molecular basis of aggregate production and their membrane interaction, it is extremely important to investigate the links between the structure of protein assemblies and the features of both their interaction with lipid membranes and their cytotoxicity. An extensive discussion on the role of lipid-protein interactions in amyloid formation is reported in a recent review (48).

Our experimental conditions were designed to study the interaction with the membrane of protein aggregates at well-defined aggregation states. The duration of the experiments on monolayers and supported bilayers is small compared to the typical timescales of the aggregation process of HypF-N (approximately 10 days are required at a concentration of 30% TFE to obtain mature fibrils). Although the presence of the lipid surface may accelerate the aggregation process (48), it is reasonable to assume that within this time lapse, protein aggregates do not undergo significant changes other than those caused by the interaction with the lipid moiety. Moreover, experiments in situ, as those reported in Fig. 6, show that the step-height distribution does not change with time, whereas the domain size increases, indicating that bilayer destabilization proceeds even in the absence of a protein reservoir. A different scenario is found for monomeric HypF-N. In this case, the lipid moiety lowers the activation energy barrier for protein unfolding, which in turn induces an extensive insertion of the protein in lipid monolayers and a strong destabilization of lipid bilayers.

We observed that the HypF-N domain exhibits a significant surface activity even in its native state, where it forms a monolayer upon adsorption at the air/water interface, as shown in Fig. 1, *a* and *b*. This behavior is likely due to the increased hydrophobicity of the domain as a result of its partial unfolding. In fact, the exposure of the protein molecules to the asymmetrical energetic balance after adsorption at the air/water interface results in surface-induced structural unfolding (15). This effect had already been observed in early experiments (49) and has recently been reported for other proteins involved in amyloid formation, such as lactoferrin

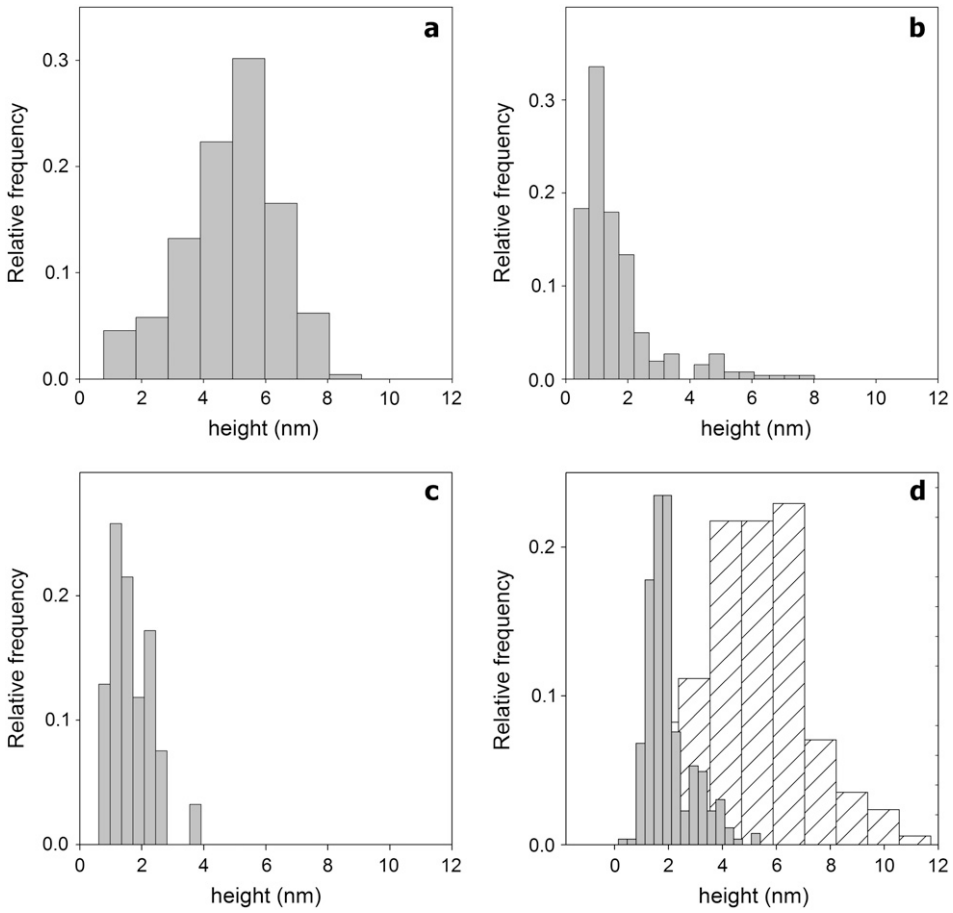

FIGURE 8 Histogram of PS membrane step height measured from surface profiles (*a*) without HypF-N, and after incubation with (*b*) native HypF-N, (*c*) HypF-N aggregated for 48 h, and (*d*) HypF-N aggregated for 72 h (*gray*) and 13 days (*cross-hatched bars*).

(50). Additional evidence supporting the increased hydrophobicity of HypF-N at the air-water interface is the strong interaction of the monomeric protein with PC or PS monolayers. In the presence of HypF-N, the isotherms of both PC and PS monolayers are considerably expanded as a consequence of protein insertion into the monolayer, with a much larger expansion in PS than in PC monolayers. The latter finding suggests that a higher number of protein molecules are recruited by the PS monolayers at the interface, possibly as a consequence of electrostatic effects; the different lipid content of the monolayers could also induce a more consistent unfolding and expansion of the adsorbed protein.

In the presence of early HypF-N aggregates, PS and PC monolayers were found to behave differently: although PS isotherms were more expanded by early aggregates than by native HypF-N, the opposite behavior was observed for PC isotherms. However, in the presence of HypF-N left in the aggregation medium for longer times, both PC and PS isotherms displayed a reduced expansion effect. Overall, these results suggest that the degree of hydrophobicity of early HypF-N aggregates decreases with increasing aggregation time, in agreement with the higher instability of early aggregates compared to mature fibrils in an aqueous environment. It has been proposed that such an instability favors the interaction of early aggregates with hydrophobic surfaces and/or their reorganization into more stable higher-order polymers (1). In stable, mature amyloid fibrils, which are the final product of the process, the hydrophobic patches and the main-chain atoms exposed in the early oligomers are likely to be shielded from contact with water. Exposure of the main polypeptide chain to water weakens intra- or interchain hydrogen bonds, favoring chain insertion into a less polar environment such as the membrane interior, where it can be shielded from water contact, increasing the strength of polar interactions (20).

The larger expansion effects observed in PS monolayers indicate that, in addition to hydrophobic effects, electrostatic interactions also play an important role in favoring protein insertion into the lipid moiety. Many recent articles support a role of anionic surfaces (mica, SDS micelles, synthetic bilayers enriched in anionic phospholipids, or other biological polymers) in favoring protein recruitment, unfolding, and aggregation (7,8,11,12,24); negative charges have also been shown to be key sites where early aggregates of different proteins and peptides interact with synthetic and cell membranes (9,51,52).

Our results indicate that the surface morphology of supported bilayers is strongly affected by the presence of

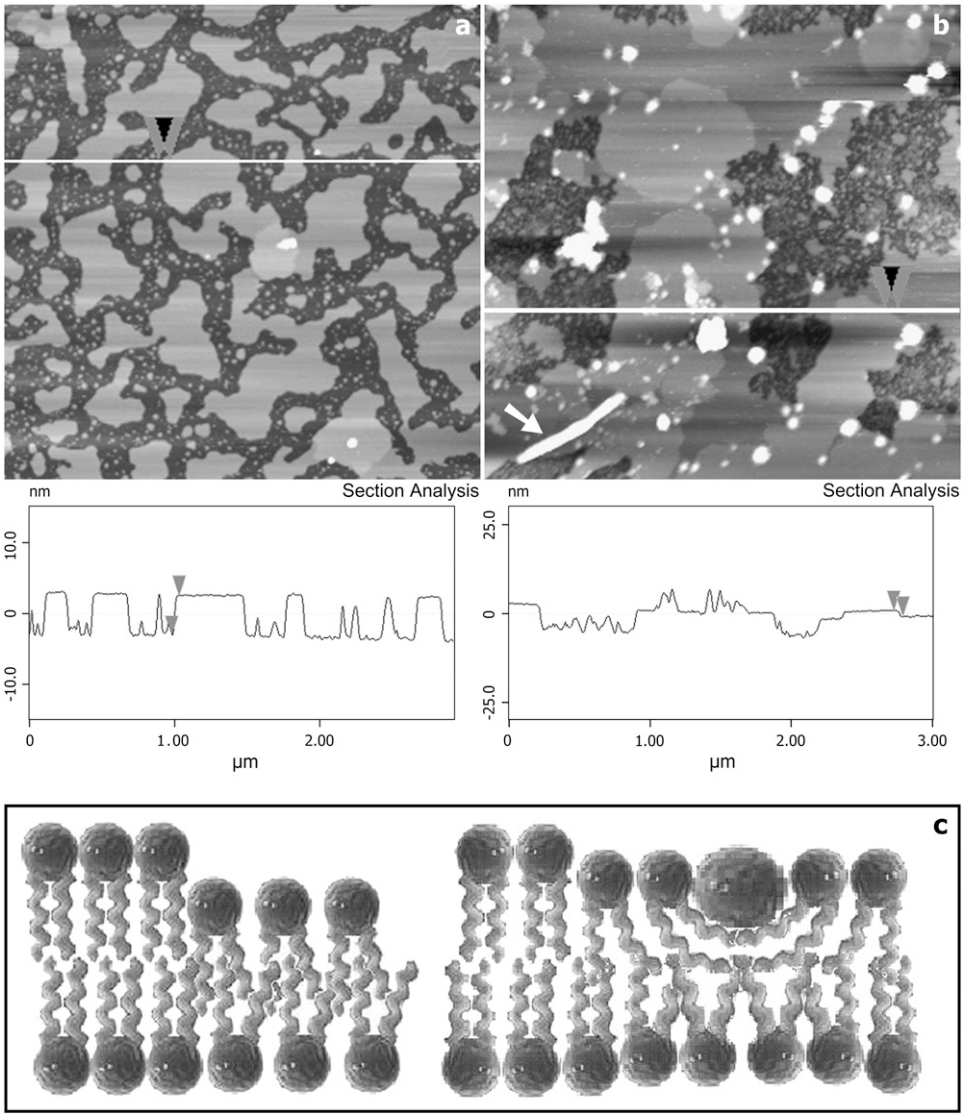

FIGURE 9 Tapping-mode atomic force microscopy images (height data) of supported membranes made of PS (*a*) without HypF-N; and (*b*) after incubation with HypF-N preaggregated for 13 days. Scan size, 3 μm; *z* range, (*a*) 30 nm; (*b*) 60 nm. Image sections performed along the lines indicated in the figures are also reported. (*c*) Cartoon showing the difference in bilayer thickness that arises from the formation of a thinner phase, resulting in small steps in the topography of the supported layers. Two different models of membrane thinning are shown (see Discussion).

HypF-N. The latter is incorporated into the lipid moiety, as shown by the antibody binding experiments, and therefore appears directly involved in membrane structural changes. After the strong interaction of native HypF-N with lipids, the structure of PC bilayers appears extensively altered, displaying regions of granular appearance. In this case, the lipid rearrangement corresponds to a sort of micellization; when this occurs, it becomes impossible to measure the thickness of the bilayer, as the latter is completely lost. A similar behavior, resulting in granular lesions of the bilayer, has already been observed in the presence of human amylin (36). Another typical feature observed as a result of the interaction of HypF-N with supported bilayers is the occurrence, in the bilayers, of steps whose height is well below the thickness of the bilayer itself. In fact, the protein-lipid interaction causes depletion of the bilayer lipids in a manner similar to that associated with the effect of surfactants, allowing the formation of a thinner phase. The reduced step heights are likely to correspond to differences between the thickness of standard bilayers and that of the thinner phase, as shown in the cartoon in Fig. 9 *c*. A possible explanation of membrane thinning could be the formation of an interdigitated phase. However, interdigitated phase formation as a consequence of peptide interaction with the membrane has been described for gel-phase bilayers (53,54), whereas our experiments have been performed above the lipid transition temperature. An alternative explanation of membrane thinning was described by Huang (55,56) for amphiphilic antimicrobial peptides. The peptide insertion in the interfacial region of a fluid bilayer causes the expansion of the headgroup region laterally. This causes the hydrocarbon chains to undergo *trans-gauche* conformational changes to accommodate the lateral expansion. As the chain volume does not change significantly when the chain conformation switches from *trans* to *gauche*, the average thickness of the bilayer decreases.

Membrane disruption induced by HypF-N exhibits different features in PS and PC supported bilayers. Indeed, changes in step height are measured in both systems, although micellization effects appear to predominate in PC bilayers. In the case of PS bilayers, the height distributions show the persistence of a small fraction of unperturbed lipids, whereas this finding disappears in PC bilayers. This behavior could be a consequence of the different ratio of saturated to unsaturated fatty acids in either lipid (0.88 for PC and 0.95 for PS), which could more easily result in phase separation for PS bilayers. In addition, as pointed out above, electrostatic effects could also play a role in protein-PS bilayer interactions.

It has been proposed that cytotoxic effects of amyloid aggregates can initially be traced back to alteration of ionic equilibria inside exposed cells due to membrane permeabilization. This event could occur either through the organization of the monomers into membrane-spanning oligomeric pores with poor ion specificity (57) or through the formation of bilayer defects spreading over the entire membrane surface and leading to local membrane disruption (27). In our investigation, we did not observe porelike structures in the bilayer. On the other hand, previous studies suggested that interdigitation, or, more generally, membrane thinning, is not induced by peptides that insert across the membrane but, rather, appears to result from lateral separation of lipid headgroups by the peptides (58). Therefore, the previously reported membrane permeabilization by HypF-N aggregates (38) is likely to occur in regions where the latter form diffuse defects as a consequence of either micellization effects or bilayer thinning. In addition, the adsorption of monomers or oligomers on the surface of lipid bilayers at sites where the thickness is reduced could produce protein-facilitated electroporation with a mechanism similar to that proposed for annexin V (59).

It might be surprising that even native HypF-N displays such a strong interaction with lipid monolayers and bilayers. However, the presence of a lipid surface can favor protein unfolding (60) in the same way that the air/water interface can (50). The effect of a surface in favoring protein recruitment, unfolding, and aggregate nucleation can depend on the molecular and physicochemical features of either the protein or the membrane itself. It is known that in the adsorbed state proteins may undergo structural modifications involving nonnative interactions of specific residues. Accordingly, functional (most often hydrophobic) groups can be exposed on the surface without paying the energy penalty of exposing the same groups to the aqueous environment (15), thus lowering the activation energy barrier for protein unfolding. The surface chemical and physicochemical features affecting the conformational states of adsorbed proteins include surface chemistry and charge, wettability, thickness, and curvature (21,61). Therefore, in the presence of a lipid interface the structure of monomeric HypF-N most likely cannot be defined as ''native'' anymore, even though we have not assessed the type and extent of its structural perturbation.

A question that arises is whether the protein undergoes further aggregation steps as a consequence of the interaction with the membrane. Our experimental conditions were designed with the aim of controlling the protein aggregation state. Protein aggregates after TFE removal were incubated on the membrane for 20 min, after which the sample was washed before AFM inspection. As the typical time scales of the aggregation process are much longer (approximately 10 days are required at a concentration of 30% TFE to obtain mature fibrils), it is reasonable to assume that the aggregation process did not proceed further.

Overall, the data obtained with monolayers and supported bilayers agree in indicating a strong interaction of natively folded monomeric HypF-N and its early aggregates with the lipid moiety. In fact, both monomeric HypF-N and its early aggregates insert into lipid monolayers and bilayers, giving rise to isotherm expansion and extensive changes in bilayer morphology, whereas mature fibrils produced only minor effects on both model systems.

An increasing number of studies are focused at providing information on the effects of surfaces, notably synthetic or biological membranes, on protein/peptide recruitment, local concentration, misfolding, and aggregate nucleation (8,17, 19,23,62). From these studies, it is becoming increasingly apparent that biological surfaces are key triggers of amyloid aggregation and/or aggregate cytotoxicity and that the latter depends on the composition of the surfaces themselves. Our data add to those of many others in trying to describe the physicochemical features underlying peptide/protein interaction with membranes, an increasingly recognized key feature of amyloid toxicity.

We thank Silvia De Stefano for help in AFM data elaboration.

This work was supported by grants from the Italian Ministero dell'Università della Ricerca (2004050405, 2005053998, and RBNE01S29H) and the Fondazione Cassa di Risparmio di Genova.

REFERENCES

1. Stefani, M., and C. M. Dobson. 2003. Protein aggregation and aggregate toxicity: new insights into protein folding, misfolding diseases and biological evolution. *J. Mol. Med.* 81:678–699.
2. Dobson, C. M. 2001. The structural basis of protein folding and its links with human disease. *Phil. Trans. R. Soc. Lond. B.* 356:133–145.
3. Bucciantini, M., E. Giannoni, F. Chiti, F. Baroni, L. Formigli, J. Zurdo, N. Taddei, G. Ramponi, C. M. Dobson, and M. Stefani. 2002. Inherent toxicity of aggregates implies a common mechanism for protein misfolding diseases. *Nature.* 416:507–511.
4. Richardson, J. S., and D. C. Richardson. 2002. Natural β-sheet proteins use negative design to avoid edge-to-edge aggregation. *Proc. Natl. Acad. Sci. USA.* 99:2754–2759.
5. Rousseau, F., L. Serrano, and J. W. H. Schymkowitz. 2006. How evolutionary pressure against protein aggregation shaped chaperone specificity. *J. Mol. Biol.* 355:1037–1047.
6. Sherman, M. Y., and A. L. Goldberg. 2001. Cellular defenses against unfolded proteins: a cell biologist thinks about neurodegenerative diseases. *Neuron.* 29:15–32.

7. Necula, M., C. N. Chirita, and J. Kuret. 2002. Rapid anionic micelle-mediated α-synuclein fibrillization in vitro. *J. Biol. Chem.* 278:46674–46680.
8. Zhu, M., P. O. Souillac, C. Ionescu-Zanetti, S. A. Carter, and A. L. Fink. 2002. Surface-catalyzed amyloid fibril formation. *J. Biol. Chem.* 277:50914–50922.
9. Kayed, R., Y. Sokolov, B. Edmonds, T. M. McIntire, S. C. Milton, J. E. Hall, and C. G. Glabe. 2004. Permeabilization of lipid bilayers is a common conformation-dependent activity of soluble amyloid oligomers in protein misfolding diseases. *J. Biol. Chem.* 279:46363–46366.
10. Kourie, J. I., and C. L. Henry. 2002. Ion channel formation and membrane-linked pathologies of misfolded hydrophobic proteins: the role of dangerous unchaperoned molecules. *Clin. Exp. Pharmacol. Physiol.* 29:741–753.
11. Suk, J. Y., F. Zhang, W. E. Balch, R. J. Linhardt, and J. W. Kelly. 2006. Heparin accelerates gelsolin amyloidogenesis. *Biochemistry.* 45: 2234–2242.
12. Nandi, P. K., and J.-C. Nicole. 2004. Nucleic acid and prion protein interaction produces spherical amyloids which can function in vivo as coats of spongiform encephalopathy agent. *J. Mol. Biol.* 344:827–837.
13. Giorgetti, S., A. Rossi, P. Mangione, S. Raimondi, S. Marini, M. Stoppini, A. Corazza, P. Viglino, G. Esposito, G. Cetta, G. Merlini, and V. Bellotti. 2005. β2-microglobulin isoforms display an heterogeneous affinity for type I collagen. *Protein Sci.* 14:696–702.
14. Relini, A., C. Canale, S. De Stefano, R. Rolandi, S. Giorgetti, M. Stoppini, A. Rossi, F. Fogolari, A. Corazza, G. Esposito, A. Gliozzi, and V. Bellotti. 2006. Collagen plays an active role in the aggregation of β2-microglobulin under physio-pathological conditions of dialysis-related amyloidosis. *J. Biol. Chem.* 281:16521–16529.
15. Sethuraman, A., and G. Belfort. 2005. Protein structural perturbation and aggregation on homogeneous surfaces. *Biophys. J.* 88:1322–1333.
16. Arispe, N., E. Rojas, and H. D. Pollard. 1993. Alzheimer's disease amyloid β protein forms calcium channels in bilayer membranes: blockade by tromethamine and aluminium. *Proc. Natl. Acad. Sci. USA.* 89:10940–10944.
17. Kazlauskaite, J., N. Senghera, I. Sylvester, C. Vénien-Bryan, and T. J. T. Pinheiro. 2003. Structural changes of the prion protein in lipid membranes leading to aggregation and fibrillization. *Biochemistry.* 42:3295–3304.
18. Lührs, T., R. Zahn, and K. Wüthrich. 2006. Amyloid formation by recombinant full-length prion proteins in phospholipid bicelle solutions. *J. Mol. Biol.* 357:833–841.
19. Engel, M. F. M., H. Yigittop, R. C. Elgersma, D. T. S. Rijkers, R. M. J. Liskamp, B. de Kruijff, J. W. M. Höppener, and J. A. Killian. 2006. Islet amyloid polypeptide inserts into phospholipid monolayers as monomer. *J. Mol. Biol.* 356:783–789.
20. Fernandez, A., J. Kardos, L. R. Scott, Y. Goto, and R. S. Berry. 2003. Structural defects and the diagnosis of amyloidogenic propensity. *Proc. Natl. Acad. Sci. USA.* 100:6446–6451.
21. Chenal, A., G. Vernier, P. Savarin, N. A. Bushmarina, A. Gèze, F. Guillain, D. Gillet, and V. Forge. 2005. Conformational states and thermodynamics of α-lactalbumin bound to membranes: a case study of the effects of pH, calcium, lipid membrane curvature and charge. *J. Mol. Biol.* 349:890–905.
22. Yip, C. M., E. A. Elton, A. A. Darabie, M. R. Morrison, and J. McLaurin. 2001. Cholesterol, a modulator of membrane-associated Aβ-fibrillogenesis and neurotoxicity. *J. Mol. Biol.* 311:723–734.
23. Bokvist, M., F. Lindström, A. Watts, and G. Gröbner. 2004. Two types of Alzheimer's β-amyloid (1–40) peptide membrane interactions: aggregation preventing transmembrane anchoring versus accelerated surface fibril formation. *J. Mol. Biol.* 335:1039–1049.
24. Zhao, H., E. K. J. Tuominen, and P. K. J. Kinnunen. 2004. Formation of amyloid fibers triggered by phosphatidylserine-containing membranes. *Biochemistry.* 43:10302–10307.
25. Lee, G., H. B. Pollard, and N. Arispe. 2002. Annexin 5 and apolipoprotein E2 protect against Alzheimer's amyloid-β-peptide cytotoxicity by competitive inhibition at a common phosphatidylserine interaction site. *Peptides.* 23:1249–1256.
26. Zhao, H., A. Jutila, T. Nurminen, S. A. Wickström, J. Keski-Oja, and P. K. J. Kinnunen. 2005. Binding of endostatin to phosphatidylserine-containing membranes and formation of amyloid-like fibers. *Biochemistry.* 44:2857–2863.
27. Yip, C. M., and J. McLaurin. 2001. Amyloid-β peptide assembly: a critical step in fibrillogenesis and membrane disruption. *Biophys. J.* 80:1359–1371.
28. Ji, S.-R., Y. Wu, and S.-F. Sui. 2002. Cholesterol is an important factor affecting the membrane insertion of β-amyloid peptide (Aβ1–40), which may potentially inhibit the fibril formation. *J. Biol. Chem.* 277:6273–6279.
29. Bucciantini, M., G. Calloni, F. Chiti, L. Formigli, D. Nosi, C. M. Dobson, and M. Stefani. 2004. Pre-fibrillar amyloid protein aggregates share common features of cytotoxicity. *J. Biol. Chem.* 279:31374–31382.
30. Cecchi, C., S. Baglioni, C. Fiorillo, A. Pensalfini, G. Liguri, D. Nosi, S. Rigacci, M. Bucciantini, and M. Stefani. 2005. Insights into the molecular basis of the differing susceptibility of varying cell types to the toxicity of amyloid aggregates. *J. Cell Sci.* 118:3459–3470.
31. Calloni, G., N. Taddei, K. W. Plaxco, G. Ramponi, M. Stefani, and F. Chiti. 2003. Comparison of the folding processes of distantly related proteins. Importance of hydrophobic content in folding. *J. Mol. Biol.* 330:577–591.
32. Rosano, C., S. Zuccotti, M. Bucciantini, M. Stefani, G. Ramponi, and M. Bolognesi. 2002. Crystal structure and anion binding in the prokaryotic hydrogenase maturation factor HypF acylphosphatase-like domain. *J. Mol. Biol.* 321:785–796.
33. Bucciantini, M., S. Rigacci, A. Berti, L. Pieri, C. Cecchi, D. Nosi, L. Formigli, F. Chiti, and M. Stefani. 2005. Patterns of cell death triggered in two different cell lines by HypF-N pre-fibrillar aggregates. *FASEB J.* 19:437–439.
34. Lau, T.-L., E. E. Ambroggio, D. J. Tew, R. Cappai, C. L. Masters, G. Fidelio, K. J. Barnham, and F. Separovic. 2006. Amyloid-β peptide disruption of lipid membranes and the effect of metal ions. *J. Mol. Biol.* 356:759–770.
35. Ege, C., and K. Y. C. Lee. 2004. Insertion of Alzheimer's Aβ40 peptide into lipid monolayers. *Biophys. J.* 87:1732–1740.
36. Green, J. D., L. Kreplak, C. Goldsbury, X. Li Blatter, M. Stolz, G. S. Cooper, A. Seelig, J. Kistler, and U. Aebi. 2004. Atomic force microscopy reveals defects within mica supported lipid bilayers induced by the amyloidogenic human amylin peptide. *J. Mol. Biol.* 342:877–887.
37. Chiti, F., M. Bucciantini, C. Capanni, N. Taddei, C. M. Dobson, and M. Stefani. 2001. Solution conditions can promote HypF fibrillization and liposome permeabilization by protofibrils. *J. Mol. Biol.* 338:943–957.
38. Relini, A., C. Canale, S. Torrassa, R. Rolandi, A. Gliozzi, C. Rosano, M. Bolognesi, G. Plakoutsi, M. Bucciantini, F. Chiti, and M. Stefani. 2004. Monitoring the process of HypF fibrillization and liposome permeabilization by protofibrils. *J. Mol. Biol.* 338:943–957.
39. Jass, J., T. Tjärnhage, and G. Puu. 2000. From liposomes to supported planar bilayer structures on hydrophilic and hydrophobic surfaces: an atomic force microscopy study. *Biophys. J.* 79:3153–3163.
40. Reviakine, I., and A. Brisson. 2000. Formation of supported lipid bilayers from unilamellar vesicles investigated by atomic force microscopy. *Langmuir.* 16:1806–1815.
41. Hui, S. W., R. Viswanathan, J. A. Zasadzinski, and J. Israelachvili. 1995. The structure and stability of phospholipid bilayers by atomic force microscopy. *Biophys. J.* 68:171–178.
42. Winkler, R. G., J. P. Spatz, S. Sheiko, M. Moller, P. Reineker, and O. Marti. 1996. Imaging material properties by resonant tapping-force microscopy: a model investigation. *Phys. Rev. B.* 54:8908–8912.
43. Magonov, S. N., V. Elings, and M. H. Whangbo. 1997. Phase imaging and stiffness in tapping-mode atomic-force microscopy. *Surf. Sci.* 375:L385–L391.
44. Novitskaya, V., O. Bocharova, I. Bronstein, and I. V. Baskakov. 2006. Amyloid fibrils of mammalian prion protein are highly toxic to cultured cells and primary neurons. *J. Biol. Chem.* 281:13828–13836.

45. Chiti, F., M. Bucciantini, C. Capanni, N. Taddei, C. M. Dobson, and M. Stefani. 2001. Solution conditions can promote formation of either amyloid protofilaments or mature fibrils from the HypF N-terminal domain. *Protein Sci.* 10:2541–2547.

46. Burdick, D., J. Kosmoski, M. F. Knauer, and C. G. Glabe. 1997. Preferential adsorption, internalization and resistance to degradation of the major isoform of the Alzheimer's amyloid peptide, A β 1–42, in differentiated PC12 cells. *Brain Res.* 746:275–278.

47. Alarcon, J. M., J. A. Brito, T. Hermosilla, I. Atwater, D. Mears, and E. Rojas. 2006. Ion channel formation by Alzheimer's disease amyloid β-peptide (A β 40) in unilamellar liposomes is determined by anionic phospholipids. *Peptides.* 27:95–104.

48. Gorbenko, G. P., and P. K. J. Kinnunen. 2006. The role of lipid-protein interactions in amyloid-type protein fibril formation. *Chem. Phys. Lipids.* 141:72–82.

49. Gaines, G. L. 1966. Insoluble monolayers at liquid-gas interfaces. Interscience Publishers, New York.

50. Lu, J. R., S. Perumal, X. Zhao, F. Miano, V. Enea, R. R. Heenan, and J. Penfold. 2005. Surface-induced unfolding of human lactoferrin. *Langmuir.* 21:3354–3361.

51. Volles, M. J., S. J. Lee, J. C. Rochet, M. D. Shtileman, T. T. Ding, J. C. Kessler, and P. T. Lansbury. 2001. Vesicle permeabilization by protofibrillar α-synuclein: implications for the pathogenesis and treatment of Parkinson's disease. *Biochemistry.* 40:7812–7819.

52. Anderluh, G., I. Gutierrez-Aguirre, S. Rabzelj, S. Čeru, N. Kopitar-Jerala, P. Maček, V. Turk, and E. Žerovnik. 2005. Interaction of human stefin B in the prefibrillar oligomeric form with membranes. *FEBS J.* 272:3042–3051.

53. Mou, J., D. M. Czajkowsky, and Z. Shao. 1996. Gramicidin A aggregation in supported gel state phosphatidylcholine bilayers. *Biochemistry.* 35:3222–3226.

54. Rinia, H. A., R. A. Kik, R. A. Demel, M. M. E. Snel, J. A. Killian, J. P. J. M. van der Eerden, and B. de Kruijff. 2000. Visualization of highly ordered striated domains induced by transmembrane peptides in supported phosphatidylcholine bilayers. *Biochemistry.* 39:5852–5858.

55. Ludtke, S. J., K. He, and H. W. Huang. 1995. Membrane thinning caused by magainin 2. *Biochemistry.* 34:16764–16769.

56. Heller, W. T., A. J. Waring, R. I. Lehrer, T. A. Harroun, T. M. Weiss, L. Yang, and H. W. Huang. 2000. Membrane thinning effect of the β-sheet antimicrobial peptide protegrin. *Biochemistry.* 39:139–145.

57. Quist, A., I. Doudevski, H. Lin, R. Azimova, D. Ng, B. Frangione, B. Kagan, J. Ghiso, and R. Lal. 2005. Amyloid ion channels: a common structural link for protein misfolding disease. *Proc. Natl. Acad. Sci. USA.* 102:10427–10432.

58. Yip, C. M., A. A. Darabie, and J. A. McLaurin. 2002. A$-\beta$ 42$-$peptide assembly on lipid bilayers. *J. Mol. Biol.* 318:97–107.

59. Neumann, E., P. M. Siemens, and K. Toensing. 2000. Electroporative fast pore$-$flickering of the annexin V$-$lipid surface complex, a novel gating concept for ion transport. *Biophys. Chem.* 86:203–220.

60. Adams, S., A. M. Higgins, and R. A. Jones. 2002. Surface mediated folding and misfolding of proteins at lipid/water interfaces. *Langmuir.* 18:4854–4861.

61. Bowie, J. U. 2004. Membrane proteins: a new method enters the fold. *Proc. Natl. Acad. Sci. USA.* 101:3995–3996.

62. Knight, J. D., and A. D. Miranker. 2004. Phospholipid catalysis of diabetic amyloid assembly. *J. Mol. Biol.* 341:1175–1187.